

# Equilibrium Point Selection and Two Stage Optimal Control of Quadrotor Under Actuator Failure

Vidya C S  
 Robotics Research Center  
 IIT Hyderabad  
 Hyderabad, India  
 vidya.c@research.iit.ac.in

Harikumar Kandath  
 Robotics Research Center  
 IIT Hyderabad  
 Hyderabad, India  
 harikumar.k@iit.ac.in

**Abstract**—This paper presents a simple method for stabilizing the quadrotor dynamics under complete loss of one actuator using two-stage optimal control. Detailed equilibrium analysis and subsequent selection of operating point under actuator loss are provided, incorporating constraints on the maximum available thrust. A detailed simulation study using a high-fidelity nonlinear model of the quadrotor is presented showing the stability and performance of the closed-loop system under complete actuator loss, in the presence of external disturbances.

**Keywords**—fault tolerant control, quadrotor systems, equilibrium selection, two-stage feedback control, optimal control

## I. INTRODUCTION

Quadrotor systems have gained immense popularity in recent years due to their broad applications such as surveillance, search and rescue, and environmental monitoring [1]. The use of quadrotors for such critical tasks demands ensuring high levels of safety and reliability. However, due to their lack of redundancy in the control inputs, attitude dynamics under actuator failures in quadrotors are challenging to stabilize. This paper presents a simple method for stabilizing the quadrotor dynamics under complete loss of one actuator.

A fault tolerant control strategy for partial loss of actuator is investigated in [2] and [3]. Extensive research on fault detection and diagnosis, such as [4] and [5] are also available. The present strategies available for fault tolerant control (FTC) can be broadly classified into active and passive methods. Active methods such as [6] and [7] use a separate control strategy for fault cases. This is implemented after detecting the fault using sensors while passive methods like [8] and [9] implement a single robust control for both fault and non-fault situations. A passive FTC using delayed feedback and divided state feedback is implemented in [10] using sliding mode control. The uniform passive FTC for a quadrotor implemented in [11] and [12] eliminates the need of controller switching at the time of fault. However, the dynamic control allocation increases the complexity of implementation. In contrast to linear control strategies such as [13], [14], and [15] which perform linearization around an equilibrium point, non-linear control strategies like [16] which takes the complete non-linear dynamics of the system into consideration are much more computationally complex.

The controllability of the relaxed hover solutions for multicopters where the angular rate is a non-zero constant is investigated in [17]. Although the equilibrium selection method presented here uses a similar approach, an upper limit on maximum available thrust introduces bounded constraints on attitude. The method presented here is to give up the control of yaw dynamics and let the vehicle rotate with a constant angular rate which is broadly similar to the linear control strategies adopted by [15] and [13]. However unlike [15] which models the reduced kinematics of the vehicle by introducing a stationary unit vector, the proposed method simply uses roll and pitch angles and their angular rates to define the state of the vehicle with actuator fault thus eliminating the need for a full state observer. The key contributions of this paper are summarized below.

- A two-stage state feedback control law is proposed that stabilizes the attitude dynamics of the quadrotor under the complete loss of one actuator. In the proposed method, the outer loop utilizes roll and pitch angle feedback while the inner loop utilizes only roll rate and pitch rate feedback, and the uncontrollable yaw rate is kept bounded.
- Analysis of multiple attainable equilibrium points under motor failure is performed with a constraint on available thrust. The magnitude of the equilibrium pitch rate, yaw rate, and roll angle are considered for selecting the desired equilibrium point.
- A detailed numerical simulation using a high-fidelity nonlinear model of a quadrotor is provided showing the performance and stability of the proposed feedback control design under nominal conditions and with disturbances in the event of complete motor failure.

This paper is organized as follows: Section 2 presents an overview of the quadrotor dynamics. Section 3 contains the proposed method to find feasible equilibrium points within the bounds of maximum available thrust. It also contains a detailed discussion regarding the selection of a suitable operating point. Section 4 discusses the proposed control law and Section 5 contains the results obtained from the simulation using a high-fidelity nonlinear model of the system. Finally, the paper concludes with section 6.

## II. DYNAMICS OF A QUADROTOR SYSTEM

This section provides an overview of quadrotor dynamics, laying the foundation for subsequent discussions on fault-tolerant control strategies for quadrotor systems in the following sections of the paper.

Let  $[p_x, p_y, p_z]$  denote the position vector of the vehicle in three-dimensional space, where  $p_x$ ,  $p_y$ , and  $p_z$  are the Cartesian coordinates in the inertial frame. The attitude is expressed as  $[\phi, \theta, \psi]$ . The vectors  $\omega = [p, q, r]$  and  $\dot{\omega} = [\dot{p}, \dot{q}, \dot{r}]$  represent the angular rates and angular accelerations measured in body frame respectively. The rate of change of attitude measured in the inertial frame is given by equation (1).

$$\begin{bmatrix} \dot{\phi} \\ \dot{\theta} \\ \dot{\psi} \end{bmatrix} = \begin{bmatrix} 1 & \sin \phi \tan \theta & \cos \phi \tan \theta \\ 0 & \cos \phi & -\sin \phi \\ 0 & \frac{\sin \phi}{\cos \theta} & \frac{\cos \phi}{\cos \theta} \end{bmatrix} \begin{bmatrix} p \\ q \\ r \end{bmatrix} \quad (1)$$

$I = \text{diag}(I_x, I_y, I_z)$  represents the Inertia of the vehicle while  $I_p = \text{diag}(0, 0, I_{zp})$  represents the propeller moment of inertia.  $D = \text{diag}(\alpha, \beta, \gamma)$  represents a diagonal matrix containing drag terms in roll, pitch, and yaw respectively. The nonlinear differential equation governing the dynamics of the system is expressed as given in equation (2).

$$I\dot{\omega} + \omega \times (I\omega + \Sigma I_p w_i) + D\omega = \tau \quad (2)$$

where  $\tau = [\tau_x, \tau_y, \tau_z]$  represents the resultant torque along 3 axes.  $w_i$  is the angular speed of the  $i^{\text{th}}$  propeller. The relationship between resultant forces and propeller speeds for the quadrotor model in Fig. 1 is given by the equation (3).

$$\begin{bmatrix} \tau_x \\ \tau_y \\ \tau_z \\ T_\Sigma \end{bmatrix} = \begin{bmatrix} 0 & lK_f & 0 & -lK_f \\ -lK_f & 0 & lK_f & 0 \\ K_t & -K_t & K_t & -K_t \\ K_f & K_f & K_f & K_f \end{bmatrix} \begin{bmatrix} w_1^2 \\ w_2^2 \\ w_3^2 \\ w_4^2 \end{bmatrix} \quad (3)$$

where  $K_f$  and  $K_t$  are thrust and torque coefficients respectively and  $l$  is the vehicle arm length.

The equation governing the altitude dynamics is given below.

$$m\ddot{p}_z = mg - T_\Sigma \cos \theta \cos \phi \quad (4)$$

where  $T_\Sigma$  is the total thrust produced by all the motors.

## III. EQUILIBRIUM POINT SELECTION

This section presents a method to find a suitable equilibrium point (or operating point) for the vehicle under the failure of one actuator. The major factors that influence the choice of a suitable operating point are the constraints on maximum available thrust, the controllability of the shifted operating point, and the resulting tilt of the vehicle along the pitch and roll axis. The conventional equilibrium condition for hover is infeasible under the failure of one actuator. Hence we give up the control of yaw angle and keep the yaw rate a positive constant. The new equilibrium condition can be obtained from the following set of equations.

$$\dot{\omega} = 0, \quad \dot{\phi} = 0, \quad \dot{\theta} = 0, \quad \ddot{p}_z = 0 \quad (5)$$

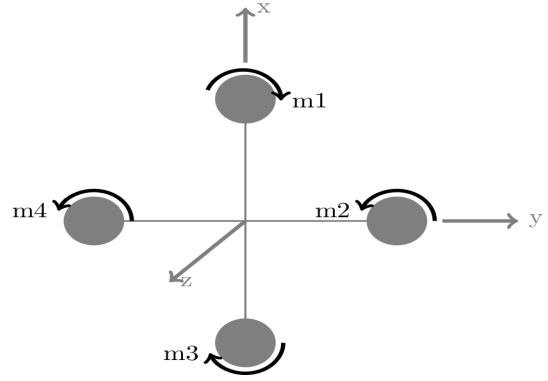


Fig. 1. Model of a quadrotor system in plus configuration. Motor 1 and motor 3 rotates in clockwise direction while motor 2 and motor 4 rotates in anticlockwise direction. Here the failure of motor 4 is discussed.

From equation (5) it can be seen that the trivial solution ( $p = 0, q = 0, \phi = 0$  and  $\theta = 0$ ) yields the following results.

$$T_1 = T_3 = \frac{mg}{2}, \quad T_2 = 0 \quad (6)$$

This indicates that the vehicle should have a minimum thrust-to-weight ratio of 2. However, this may not be possible in cases where the maximum available thrust has an upper limit. Thus assuming the fault occurs in motor 4, individual motor thrusts can be adjusted as mentioned in equation (7) to find non-trivial solutions.

$$T_1 = T_3, \quad T_2 = \lambda T_1 \quad (7)$$

where  $\lambda$  is a constant between 0 and 1. Trivial solution corresponds to the case where  $\lambda = 0$ . It is clear that for the thrust-to-weight ratio  $K < 2$ , the value of  $\lambda$  will be non-zero for all feasible solutions. Applying the relevant conditions, the equilibrium conditions obtained are given below.

$$p = 0, \quad \theta = 0, \quad r = \frac{\tau_z}{\gamma} \quad (8)$$

$$q = \frac{\tau_x}{(I_z - I_y)r - I_{zp}\Sigma w_i} \quad (9)$$

$$\phi = \tan^{-1}\left(\frac{q}{r}\right) \quad (10)$$

Note that  $p$  and  $\theta$  are zero for all feasible solutions because  $\tau_y$  is zero due to the condition mentioned in equation (7). The equilibrium point can be found by solving for the unknowns  $p, q, \phi, \theta, r, w_1, w_2, w_3$  and  $\lambda$  using the equations (5), and (7).

Multiple feasible equilibrium points can be found for a given thrust-to-weight ratio  $K$ . However, not all of them may be suitable for practical implementation. One factor to consider while selecting the operating point is the tilt of the vehicle along the roll axis. For a given  $K < 2$ , the minimum value of  $\lambda$  for which an equilibrium point can be found is denoted as  $\lambda_{min}$ . When  $\lambda = \lambda_{min}$  the torques along the roll and yaw axis are given by equation (11).

$$\tau_x = l\lambda_{min} \frac{Kmg}{4}, \quad \tau_z = K_t(2 - \lambda_{min}) \frac{Kmg}{4} \quad (11)$$

The corresponding  $q$  will be the minimum amplitude of  $q$  possible for a given  $K$ , denoted by  $q_{min}$ . Similarly, let the maximum amplitude of  $r$  be denoted by  $r_{max}$ . Substituting in equation (10), the minimum amplitude of  $\phi$  for a given  $K$  denoted by  $\phi_{min}$  is given below.

$$\phi_{min} = \tan^{-1}\left(\frac{q_{min}}{r_{max}}\right) \quad (12)$$

From equations (9), (11) and (12) it is clear that  $\phi_{min} = 0$  only for  $\lambda_{min} = 0$  which is only possible if  $K \geq 2$ .

Another factor to consider while selecting the operating point is to maximize the upward thrust and minimize the forward thrust. From equation (4), it can be seen that the steady state values of  $\theta$  and  $\phi$  greatly influence the maximum upward thrust produced. However, since every operating point generated has the steady state value of pitch angle to be zero, we only need to consider the value of  $\phi$ . Equation (13) should be satisfied to ensure the vehicle has enough upward thrust to maintain the altitude.

$$\cos(\phi) \geq \frac{1}{K} \quad (13)$$

As  $\lambda$  increases,  $q$  increases while  $r$  decreases. Hence for a given  $K$ , when  $\lambda$  is maximum,  $q$  is maximum and  $r$  is minimum. These values are denoted by  $q_{max}$  and  $r_{min}$  respectively. Similar to equation (12) a maximum amplitude of  $\phi$  for a given  $K$  denoted by  $\phi_{max}$  can be determined from equation (10). Combining the upper limit for  $\phi$  specified by equation (13),  $\phi_{max}$  is determined by the following equation.

$$\phi_{max} = \min\left(\cos^{-1}\left(\frac{1}{K}\right), \tan^{-1}\left(\frac{q_{max}}{r_{min}}\right)\right) \quad (14)$$

An operating point closer to  $\phi_{min}$  will have low forward thrust but a relatively larger yaw rate, while an operating point closer to  $\phi_{max}$  will have a considerably low yaw rate but a higher tilt along the roll axis and hence a larger forward thrust. A suitable equilibrium point can be chosen considering these factors. Moreover, the state model presented in Section 4 indicates that all equilibrium points are controllable. The detailed analysis is provided in Section 5 for a real quadrotor dynamics.

#### IV. CONTROLLER DESIGN

The controller design consists of a two-stage LQR controller for attitude control and a PID controller for altitude control as shown in Fig. 2. The outer loop of the attitude controller has pitch and roll angle feedback while the inner loop has angular rate feedback. The outer loop produces the reference values for the angular rates. The inner loop finds the required torques for following the desired state of the vehicle.

##### A. Linearized Outerloop Dynamics

The state space model for the outer loop is obtained by linearising the equations of the rate of change of roll and pitch angles measured in inertial frame ( refer equation (1) ) about the equilibrium states.

$$\dot{x}_1 = A_1 x_1 + B_1 u_1 \quad (15)$$

$$u_1 = K_1 x_1 \quad (16)$$

The state vector consists of the linearised states of roll and pitch angles represented as  $\bar{\phi}$  and  $\bar{\theta}$  which are the deviations from the equilibrium state and the input vector consists of the linearised states of roll and pitch angular rates.

$$x_1 = \begin{bmatrix} \bar{\phi} \\ \bar{\theta} \end{bmatrix}, \quad u_1 = \begin{bmatrix} \bar{p} \\ \bar{q} \end{bmatrix} \quad (17)$$

where  $\bar{\phi} = \phi - \phi_e$ ,  $\bar{\theta} = \theta - \theta_e$ ,  $\bar{p} = p - p_e$  and  $\bar{q} = q - q_e$ .  $\theta_e$ ,  $\phi_e$ ,  $p_e$  and  $q_e$  represent the equilibrium state determined using the method mentioned in section 3. Corresponding A and B matrices are given by the equations below.

$$A_1 = \begin{bmatrix} a_{11} & a_{12} \\ a_{21} & a_{22} \end{bmatrix} \quad (18)$$

where  $a_{11} = q_e \tan \theta_e \cos \phi_e - r_e \tan \theta_e \sin \phi_e$ ,  $a_{12} = (q_e \sin \phi_e + r_e \cos \phi_e) \sec^2 \theta_e$ ,  $a_{21} = -q_e \sin \phi_e - r_e \cos \phi_e$  and  $a_{22} = 0$ .

$$B_1 = \begin{bmatrix} 1 & \sin \phi_e \tan \theta_e \\ 0 & \cos \phi_e \end{bmatrix} \quad (19)$$

The optimal feedback gain  $K_1$  is determined by minimizing the cost function given by equation (20)

$$J_1 = \frac{1}{2} \int_0^\infty (x_1^T Q_1 x_1 + u_1^T R_1 u_1) dt \quad (20)$$

where  $Q_1$  is the state cost weighted matrix and  $R_1$  is the input cost weighted matrix for the outer loop. The desired values of  $p$  and  $q$  required to maintain the equilibrium states are obtained from the input vector. These values are passed on to the inner loop for determining the desired thrust and torques.

##### B. Linearized Innerloop Dynamics

The state space model for the inner loop is derived by linearising the attitude dynamics with respect to the body frame about the equilibrium states of  $p$  and  $q$ . As mentioned in the previous sections only the roll and pitch dynamics are considered while the yaw angle is kept as a free variable.

$$\dot{x}_2 = A_2 x_2 + B_2 u_2 \quad (21)$$

$$u_2 = K_2 x_2 \quad (22)$$

The state vector  $x_2$  consists of deviations of pitch and roll angular rates from the equilibrium, and the input vector  $u_2$  is a function of the deviation of actual motor thrust from equilibrium values.

$$x_2 = \begin{bmatrix} \bar{p} \\ \bar{q} \end{bmatrix}, \quad u_2 = \begin{bmatrix} \bar{T}_3 - \bar{T}_1 \\ \bar{T}_2 \end{bmatrix} \quad (23)$$

where  $\bar{T}_i = T_i - T_{ie}$  and  $T_{ie}$  represents the equilibrium thrust for  $i^{th}$  motor. Corresponding A and B matrices are given by the equations below.

$$A_2 = \begin{bmatrix} -\frac{\alpha}{I_x} & c \\ -c & -\frac{\beta}{I_y} \end{bmatrix} \quad (24)$$

$$B_2 = \frac{l}{I_x} \begin{bmatrix} 0 & 1 \\ 1 & 0 \end{bmatrix} \quad (25)$$

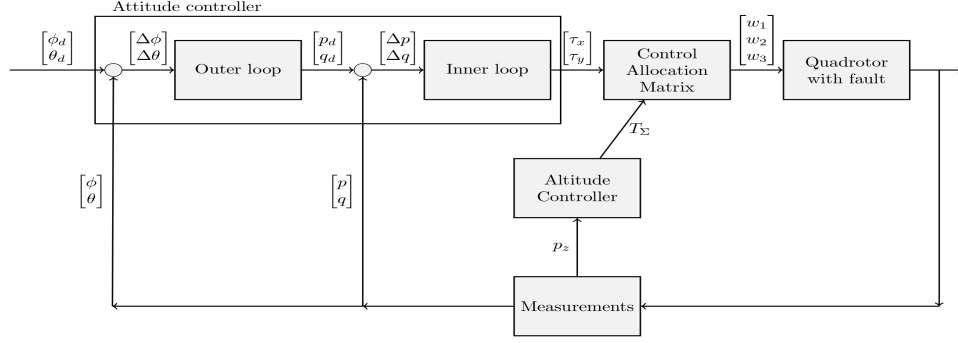


Fig. 2. Controller structure.  $\Delta$  terms indicate the error with respect to the reference value. Reference values are indicated with subscript  $d$ .

TABLE I  
VEHICLE PARAMETERS

$I_x$	$3.2 \times 10^{-3} \text{kgm}^2$
$I_y$	$3.2 \times 10^{-3} \text{kgm}^2$
$I_z$	$5.5 \times 10^{-3} \text{kgm}^2$
$I_{zp}$	$1.5 \times 10^{-5} \text{kgm}^2$
$m$	$0.5 \text{kg}$
$g$	$9.81 \text{m/s}^2$
$l$	$0.17 \text{m}$
$K_f$	$6.41 \times 10^{-6} \text{Ns}^2/\text{rad}^2$
$K_t$	$1.69 \times 10^{-2} \text{Nms}^2/\text{rad}^2$

TABLE II  
MAXIMUM AND MINIMUM VALUES OF  $\phi$  FOR THRUST TO WEIGHT RATIO  
K RANGING FROM 1.7 TO 2

K	1.7	1.75	1.8	1.85	1.9	1.95	2
$\phi_{min}(\text{deg})$	10.84	7.26	4.90	3.19	1.88	0.84	0
$\phi_{max}(\text{deg})$	30.96	35.71	39.18	42	44.4	46.5	47.72

TABLE III  
OPERATING POINTS AND THEIR CORRESPONDING PITCH AND YAW  
ANGULAR RATES FOR K = 1.8

	1	2	3	4	5
$q_e$ (rad/s)	2.06	4.6	5.6	10	12
$r_e$ (rad/s)	22.55	17.65	16.48	13.93	13.47
$\phi_e$ (deg)	4.90	13.16	16.77	32.03	37.79

where  $c = \frac{I_x - I_z}{I_x} r_e - \frac{I_{zp}}{I_x} \sum w_{ie}$ .

The optimal feedback gain  $K_2$  is determined by minimizing the cost function given by equation (26).

$$J_2 = \frac{1}{2} \int_0^{\infty} (x_2^T Q_2 x_2 + u_2^T R_2 u_2) dt \quad (26)$$

where  $Q_2$  is the state cost weighted matrix and  $R_2$  is the input cost weighted matrix for the inner loop.

### C. Altitude Controller

The altitude controller has a PID structure of the following form.

$$\bar{T} = K_p e + K_i \int e + K_d \frac{de}{dt} \quad (27)$$

where  $\bar{T} = T_{\Sigma} - T_h$  represents the deviation in total thrust from desired hover thrust and  $e = p_z - p_{ze}$  represents the error in altitude.  $T_h$  represents the desired hover thrust.

$$T_{\Sigma} = T_1 + T_2 + T_3 \quad (28)$$

From equations (23) and (28), the individual thrust required for each of the remaining motors can be computed.

## V. RESULTS

This section presents the results obtained for the equilibrium analysis and subsequent simulation results for a vehicle with parameters specified in Table I [15].

### A. Equilibrium point selection

The equilibrium point is obtained for given values of  $p$  and  $q$  where  $p$  is kept 0 since all equilibrium solutions have  $p = 0$  as mentioned in section 3. Fig. 3 and Fig. 4 show some arbitrarily selected periodic solutions for corresponding values of  $K$ . It can be seen that for a thrust-to-weight ratio below 1.7, no feasible solutions are obtained. For a given  $K$ , as the value of  $q$  increases, the  $r$  obtained decreases. Thus if we want to lower the yaw rate, there will be an increase in the value of  $\phi$  which indicates an increase in forward thrust. If we disregard the constraint that the two motor speeds should be equal, many more periodic solutions can be found. Table II shows the maximum and minimum values of  $\phi$  obtained for different values of  $K$  ranging from 1.7 to 2. It should be noted that for each  $K$ , these obtained values correspond to the range specified in section 3. As mentioned in Section 3, the  $\phi$  must be minimized to minimize the forward thrust. For a thrust-to-weight ratio of 1.8, a comparison of  $q$ ,  $r$ , and  $\phi$  values of a few operating points is shown in Table III. From here it can be seen that the possible minimum value of  $\phi$  is 4.9 degrees. Hence this equilibrium point is chosen for operation.

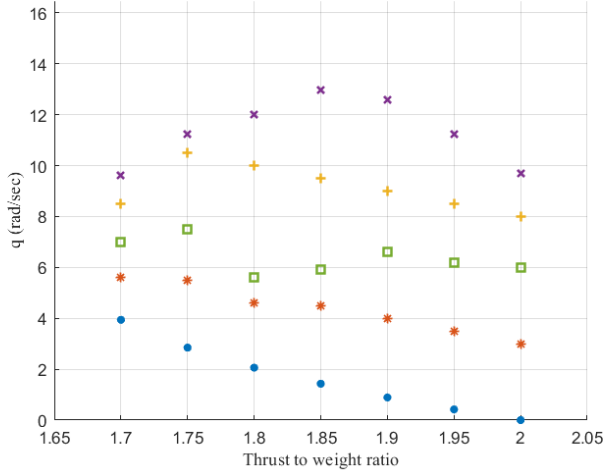


Fig. 3. Arbitrarily selected operating points for  $K = 1.7$  to  $K = 2$  and corresponding pitch rates

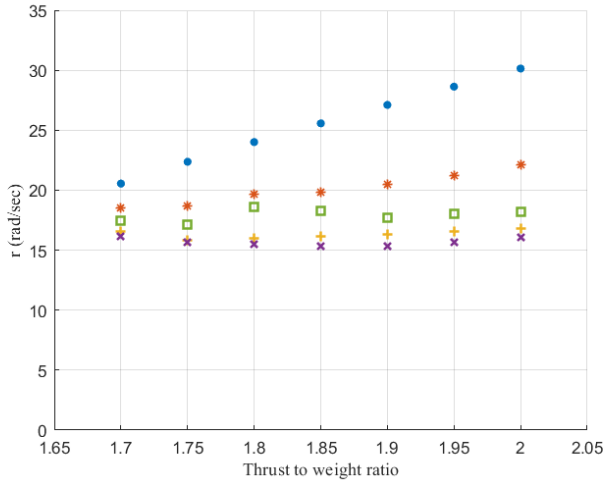


Fig. 4. Yaw rates corresponding to the operating points plotted in Fig. 3. For a fixed  $K$ , the same color indicates the same operating point

### B. Simulation Results

This section presents the results obtained by simulating the proposed method with a high-fidelity nonlinear model in MATLAB with added disturbances. The  $D$  matrix containing drag terms in roll, pitch, and yaw are assumed to be  $diag(0.2, 0, 0.00275)$ . The equilibrium parameters of the vehicle for the selected operating point are given in Table IV. The cost weight matrices for the outer loop and inner loop are chosen considering the convergence of the inner loop should be faster than the outer loop. The closed loop poles of the outer loop are  $-0.547 + 24.1i$  and  $-0.547 - 24.1i$  while the closed loop poles of the inner loop are  $-108.434$  and  $-25.612$ .

The system model is simulated for a total of 40s. The fault occurs at  $t = 1s$  resulting in the complete failure of motor 4, which is indicated by a red vertical line in the

TABLE IV  
PARAMETERS OF THE SELECTED OPERATING POINT

$r_e$ (rad/s)	$\phi_e$ (deg)	$\theta_e$ (deg)	$w_{1e}$ (rad/s)	$w_{2e}$ (rad/s)	$w_{3e}$ (rad/s)	$\lambda$
24.01	4.90	0	586.8090	281.1545	586.8090	0.2297

plots. The system is shifted to the desired equilibrium point by only adjusting the motor inputs at the instant of fault. The controller is turned on only when the deviation from the desired equilibrium state is within the tolerable limits. Here that is found to be  $t = 1.1s$  which is after 10 time steps. As observed in Fig. 6 and Fig. 7 the angular rates and altitude of the system completely stabilize within 20 sec. The steady-state error in altitude is found to be within  $\pm 1.2\%$ .

A rectangular pulse with a magnitude of about 3 times the original value and a width of 2 time steps is introduced in the motor 1 input for simulating an external disturbance (refer to Fig. 5) at  $t = 20s$ . The results obtained for this case are plotted in Fig. 6 and Fig. 7 respectively. There is a significant deviation from the equilibrium point at the moment of disturbance in angular rates. However, it immediately stabilizes as observed in Fig. 6. This can be further observed in Fig. 7 where the oscillations caused by the disturbance almost completely die within 10s.

The assumed case here is that the vehicle can detect fault the moment it occurs. However, this is not achievable in practice. This is investigated by introducing a time lag between the time instance of the fault occurrence, and the time instance of shifting to the desired equilibrium point. It is found that even with a lag of 30 samples, the system can stabilize to the desired equilibrium point. However as the lag increases, there is a slight increase in steady state error in altitude  $z$  and yaw rate  $r$ . The sampling time taken here is 0.01s. The system can stabilize with a steady state error of  $\pm 5\%$  even with a lag of 0.3 seconds in detecting the fault.

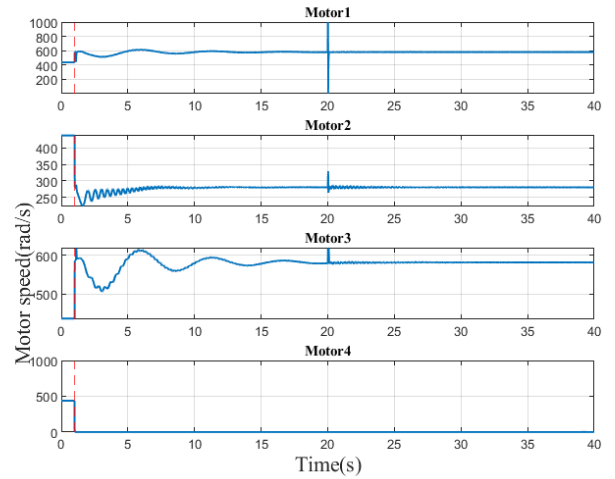


Fig. 5. Motor inputs with external disturbances

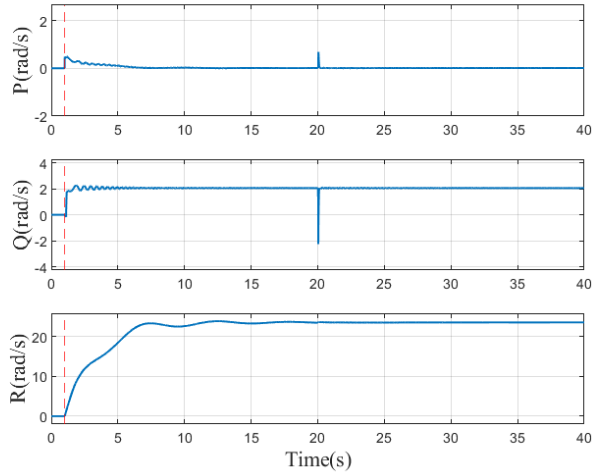


Fig. 6. Angular rates obtained in simulation corresponding to the motor inputs in Fig. 5

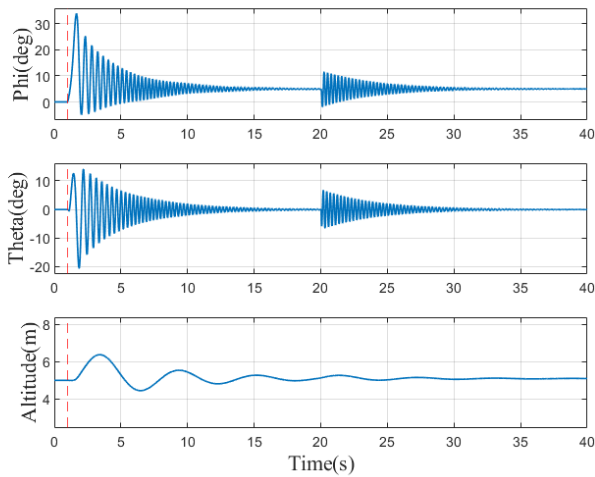


Fig. 7.  $\theta$ ,  $\phi$  and altitude  $p_z$  obtained in simulation corresponding to the motor inputs in Fig. 5

## VI. CONCLUSIONS

In this paper, a method for stabilizing the quadrotor dynamics under complete loss of one actuator is presented. The proposed method gives up the control of the yaw angle and uses a two-stage optimal control for stabilizing the vehicle. A detailed analysis of equilibrium selection under thrust constraints presented here indicates that stabilization is possible for the lowest thrust-to-weight ratio of 1.7. The analysis also indicates the effect of the direction of thrust and the tilt of the vehicle on the choice of equilibrium point. The use of a two-stage LQR controller with only  $p$  and  $q$  feedback in the inner loop and  $\theta$  and  $\phi$  feedback in the outer loop reduces the relative computational complexity in implementation. The proposed method is verified through simulation with a high-fidelity non-linear model. The results indicate that the system

is stable even with disturbances in motor inputs, and can also tolerate a time lag in fault detection up to 0.3 seconds.

## ACKNOWLEDGMENT

The authors acknowledge the financial support given by TiHAN, IIT Hyderabad under the project number TiHAN-IITH/03/2021-22/33(4).

## REFERENCES

- [1] Josy John, K. Harikumar, J. Senthilnath, and Suresh Sundaram. An efficient approach with dynamic multiswarm of uavs for forest firefighting. *IEEE Transactions on Systems, Man, and Cybernetics: Systems*, 54(5):2860–2871, 2024.
- [2] Mina Ranjbaran and Khashayar Khorasani. Fault recovery of an under-actuated quadrotor aerial vehicle. In *49th IEEE conference on Decision and Control (CDC)*, pages 4385–4392. IEEE, 2010.
- [3] Xuerui Wang, Sihao Sun, Erik-Jan van Kampen, and Qiping Chu. Quadrotor fault tolerant incremental sliding mode control driven by sliding mode disturbance observers. *Aerospace Science and Technology*, 87:417–430, 2019.
- [4] M Hadi Amoozgar, Abbas Chamseddine, and Youmin Zhang. Experimental test of a two-stage kalman filter for actuator fault detection and diagnosis of an unmanned quadrotor helicopter. *Journal of Intelligent & Robotic Systems*, 70:107–117, 2013.
- [5] Alessandro Freddi, Sauro Longhi, and Andrea Monteriu. Actuator fault detection system for a mini-quadrotor. In *2010 IEEE International Symposium on Industrial Electronics*, pages 2055–2060. IEEE, 2010.
- [6] Peng Lu and Erik-Jan van Kampen. Active fault-tolerant control for quadrotors subjected to a complete rotor failure. In *2015 IEEE/RSJ International Conference on Intelligent Robots and Systems (IROS)*, pages 4698–4703. IEEE, 2015.
- [7] Ban Wang, Yanyan Shen, and Youmin Zhang. Active fault-tolerant control for a quadrotor helicopter against actuator faults and model uncertainties. *Aerospace Science and Technology*, 99:105745, 2020.
- [8] Hasan Başak, Emre Kemer, and Emmanuel Prempain. A passive fault-tolerant switched control approach for linear multivariable systems: Application to a quadcopter unmanned aerial vehicle model. *Journal of Dynamic Systems, Measurement, and Control*, 142(3):031004, 2020.
- [9] Abdel-Razzak Merheb, Hassan Noura, and François Bateman. Design of passive fault-tolerant controllers of a quadrotor based on sliding mode theory. *International Journal of Applied Mathematics and Computer Science*, 25(3), 2015.
- [10] Safi Ullah, Kamran Iqbal, and Fahad Malik. Fault-tolerant sliding mode control of a quadrotor uav with delayed feedback. *International Journal of Mechanical Engineering and Robotics Research*, 12 2019.
- [11] Chenxu Ke, Kai-Yuan Cai, and Quan Quan. Uniform passive fault-tolerant control of a quadcopter with one, two, or three rotor failure. *IEEE Transactions on Robotics*, 39(6):4297–4311, 2023.
- [12] Chenxu Ke, Kai-Yuan Cai, and Quan Quan. Uniform fault-tolerant control of a quadcopter with rotor failure. *IEEE/ASME Transactions on Mechatronics*, 28(1):507–517, 2023.
- [13] Alessandro Freddi, Alexander Lanzon, and Sauro Longhi. A feedback linearization approach to fault tolerance in quadrotor vehicles. *IFAC proceedings volumes*, 44(1):5413–5418, 2011.
- [14] Vincenzo Lippiello, Fabio Ruggiero, and Diana Serra. Emergency landing for a quadrotor in case of a propeller failure: A pid based approach. In *2014 IEEE International Symposium on Safety, Security, and Rescue Robotics (2014)*, pages 1–7. IEEE, 2014.
- [15] Mark W Mueller and Raffaello D’Andrea. Stability and control of a quadcopter despite the complete loss of one, two, or three propellers. In *2014 IEEE international conference on robotics and automation (ICRA)*, pages 45–52. IEEE, 2014.
- [16] Fang Nan, Sihao Sun, Philipp Foehn, and Davide Scaramuzza. Nonlinear mpc for quadrotor fault-tolerant control. *IEEE Robotics and Automation Letters*, 7(2):5047–5054, 2022.
- [17] Mark W. Mueller and Raffaello D’Andrea. Relaxed hover solutions for multicopters: Application to algorithmic redundancy and novel vehicles. *The International Journal of Robotics Research*, 35(8):873–889, 2016.